Q switching and mode locking pulse generation from an all-fiber ring laser by intermodal acousto-optic bandpass modulation

E Hernández-Escobar[1], M Bello-Jiménez[1], R López-Estopier[1,2], A Camarillo-Avilés[1], O Pottiez[3], M A García-Ramírez[4], M Durán-Sánchez[2,5], B Ibarra-Escamilla[5] and M V Andrés[6]

[1]Instituto de Investigación en Comunicación Óptica (IICO), Universidad Autónoma de San Luis Potosí, Av. Karakorum No. 1470 Lomas 4ª Secc., 78210 San Luis Potosí, México
[2]Consejo Nacional de Ciencia y Tecnología (CONACYT), Av. Insurgentes Sur No. 1582, Col. Crédito Constructor, Del. Benito Juárez, México, D.F. 039040, México
[3]Centro de Investigaciones en Óptica (CIO), Loma del Bosque No. 115, Col. Lomas del Campestre, León, Guanajuato 37150, México
[4]Universidad de Guadalajara, Research Centre for Applied Sciences and Engineering (CUCEI), Electronics and Computer Sciences Dep. Blvd. Marcelino García Barragán No. 1421, Esq. Calzada Olímpica, 44430, Guadalajara, Jalisco, México
[5]Instituto Nacional de Astrofísica, Óptica y Electrónica (INAOE), Luis Enrique Erro No 1, Departamento de Óptica, 72000 Puebla, México
[6]Universidad de Valencia, Departamento de Física Aplicada y Electromagnetismo, ICMUV, c/Dr. Moliner 50, Burjassot, 46100 Valencia, Spain

E-mail: miguel.bello@uaslp.mx

Abstract. Q-switched and mode-locked (QML) pulse generation from an all-fiber ring laser based on intermodal acousto-optic bandpass modulation is reported. The modulator relies on full-acousto-optic mode re-coupling cycle induced by a standing flexural acoustic wave, with a transmission response that is controlled by amplitude modulation of the acoustic wave signal. The Q factor of the cavity is controlled by a rectangular pulse wave with variable frequency and duty cycle, whereas mode locking is achieved by amplitude modulation derived from a standing flexural acoustic wave. The best QML pulses were obtained at 0.5 kHz repetition rate, with a pump power of 549.2 mW, at the optical wavelength of 1568.2 nm. A maximum overall energy of 2.14 μJ at an average output power of 1.07 mW was achieved, corresponding to a burst of mode-locked sub-pulses of 100 ps pulse duration within a QML envelope of 3.5 μs.

Keywords: Q-switched and mode-locked**,** Fiber lasers, Acousto-optic modulation, Fiber optics.

1. Introduction

Pulsed fiber lasers have emerged as essential optical light sources for a wide variety of photonic applications [1-5]. For applications involving short or ultrashort pulse generation, mode locking is the preferred technique, whereas for applications that comprise relatively long and highly energetic optical pulses, Q switching is the most suitable technique. In this respect, a different type of pulsed regime, called Q-switched mode locking (QML), has been proposed and demonstrated to combine the inherent advantages of mode locking and Q switching techniques in order to produce a burst of high-intensity mode-locked optical pulses within a long Q-switching envelope [6-10]. Pulse operation in the QML regime is obtained either with passive or active techniques [6-13], or a hybrid combination of them [14-16]. Passive configurations are regarded as being the simplest schemes, without including an external signal source and the capacity of generating short or ultrashort internal sub-pulses [8-12,17,18]. Notwithstanding, a major shortcoming is the

limited control over the output pulses parameters and a fixed repetition rate. In contrast, active schemes possess the advantages of tight control over intracavity parameters, enabling improvements on the output pulse characteristics [6,7,13,19]. However, their major drawback is the relatively long pulse generation associated with the limited optical bandwidth of the active device. Consequently, one of the most common method for QML pulse generation relies on ultrashort pulse generation based on a passive mode locker, together with an active Q-switching operation [20-23].

In the framework of QML all-fiber lasers, the development of efficient in-fiber modulators is of great interest. In the past few years, there have been many efforts in this direction, and a few in-fiber approaches have been reported [24-30]. In this regard, our group has previously investigated a novel type of in-fiber acousto-optic (AO) tunable bandpass modulator, whose operation principle relies on full-acousto-optic mode re-coupling cycle induced by flexural acoustic waves. By using this AO device, Q-switched [31] and mode-locked [32] pulse operation was successfully obtained. Now, with the goal of producing a stable QML pulse emission, the modulator is operated to allow simultaneous emission of QML optical pulses. In this way, the AO modulator performs the double function of active mode locker and Q-switching device. This work, to the best of our knowledge, is the first approach describing a doubly active QML all-fiber laser based on the acousto-optic effect produced by flexural acoustic waves in an optical fiber.

In this paper we present an experimental investigation regarding a dual actively Q-switched mode-locked all-fiber light source by implementing an in-fiber acousto-optic bandpass modulator (AOBM). Intracavity loss modulation is controlled by modulation of the acoustic wave signal. When the acoustical signal is switched on, a standing flexural acoustic wave is formed on the modulator, and the transmission is amplitude modulated at two times the frequency of the acoustic wave. Therefore, by precisely matching the modulation period and the cavity round-trip time, the mode locking condition is satisfied. At the same time, superimposing a rectangular wave modulation on the acoustic signal, intermittent periods of light are generated, allowing control of the Q factor of the cavity. In this manner, QML pulse operation is controlled by variations in the frequency and duty cycle of the modulating rectangular signal. Experimental results demonstrate the potential of the proposed scheme, and provide useful information for future optimization of in-fiber AO devices. Besides this, our approach preserves the simplicity and robustness required in all-fiber arrangements.

2. Experimental setup

The setup of the all-fiber laser is shown in figure 1(a). The gain fiber is a 0.8-m-long Er/Yb co-doped double-cladding fiber (CorActive, DCF-EY-10/128) pumped by a pigtailed multimode laser diode emitting at 976 nm. The pump radiation is delivered via a (2+1)×1 fiber combiner. Then, an in-line polarization controller (PC) is included to adjust the polarization state before the acousto-optic modulator (AOM). The modulator is connected after the PC and is followed by a 50/50 fiber coupler. The coupler provides the output light pulses and is connected to a delay line. The delay line is required to match the cavity round-trip time with the modulation period. A fiber isolator is incorporated to ensure unidirectional operation within the ring cavity. Finally, the cavity is closed by splicing the fiber isolator to the signal port of the pump combiner. In relation to cavity dispersion (D), all fiber components, with the only exception of the active fiber, are composed of Corning SMF-28 fiber. Thus, the cavity dispersion is anomalous.

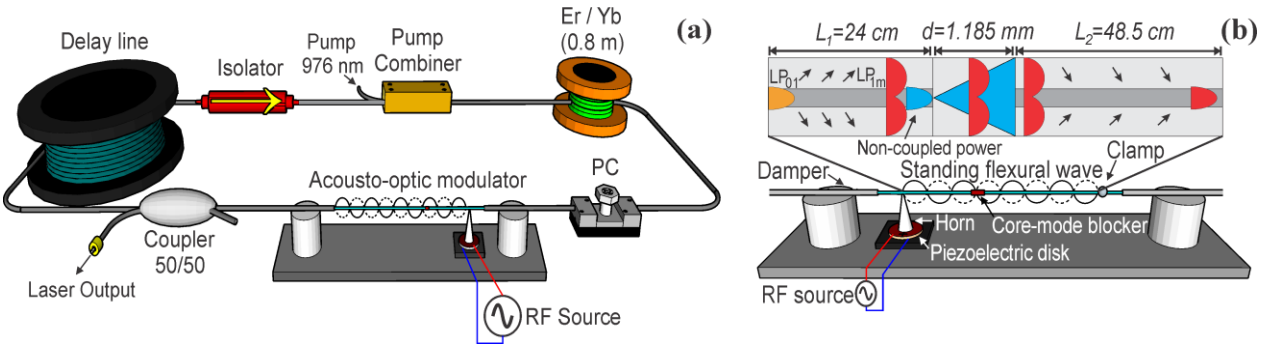

Figure 1. (a) Schematic setup of the mode-locked fiber ring laser. (b) Acousto-optic modulator.

A schematic view of the AOM and its operation principle is shown in figure 1(b). The modulator consists on the same experimental arrangement described in Refs. [31, 32]. Here, and for reasons of clarity, only the main transmission characteristics are described. For a detailed characterization of the modulator, please see the references above. As illustrated in figure 1(b), the length of the section of fiber L_1 is selected to allow the fundamental mode to be coupled to a cladding mode previous the core-mode blocker (CMB), whereas the length of fiber L_2 is selected to achieve the highest reinsertion of energy between the cladding and the core modes. The lengths of fibers L_1 and L_2 were set to 24 and 48.5 cm, respectively. The length d of the CMB, which consists of a short section of coreless optical fiber (Thorlabs FG125LA), is calculated for the light leaving the section of fiber L_1 to be expanded over the front face of the fiber L_2. With an effective index of 1.446 for the fundamental mode at a wavelength of 1550 nm, and a refractive index of 1.444 for the coreless fiber, d is calculated as 1.185 mm. The modulator is finally completed with a radio frequency (RF) source, a ceramic piezoelectric disk (PD) and an aluminum concentrator horn. The transmittance of the CMB in the absence of acoustic wave is shown in figure 2(a). This measurement was realized by illuminating the AOM with a tunable laser diode (1520 – 1570 nm) and detecting the transmitted signal with an optical power meter. This result demonstrates a strong suppression of light by at least 20.2 dB in a range of wavelengths between 1520 and 1570 nm, with a maximum attenuation of 25.2 dB at 1537 nm. On the other hand, and under the effect of a traveling flexural acoustic wave, the modulator is capable to bypass the CMB via cladding propagation. The bandpass characteristics of the modulator are depicted in figure 2(b). The strongest AO resonance was found at the acoustic frequency (f_a) of 2.427 MHz for a voltage applied to the piezoelectric disk (V_{PD}) of 28.6 V (hereinafter, the voltage is a peak-to-peak measurement). The 3-dB optical bandwidth is 0.91 nm with minimum insertion loss of 2.7 dB at the resonant optical wavelength (λ_R) of 1569.6 nm. Then, with the aim of producing a bandpass amplitude modulation, the fiber end opposite to the aluminum horn is immersed in a drop of welding. This produces the reflection of the acoustic wave, and a standing flexural acoustic wave is established along the modulator. Consequently, the transmission oscillates in time at twice the frequency of the acoustic signal. Figure 2(c) shows the transmitted light as a function of time when a RF signal of 2.427 MHz and 28.6 V is applied to the piezoelectric disk. For this measurement, the modulator is illuminated at the resonant optical wavelength of 1569.6 nm and the transmitted light is monitored with a standard oscilloscope. An amplitude modulation at 4.8473 MHz is clearly visible, which is two times the frequency of the piezoelectric voltage (V_{PZT}). From this result, the insertion loss is measured as 3.71 dB together with a modulation depth of 0.77. The time response of the modulator is also shown in figure 2(d). For this measurement, a rectangular signal is superimposed in order to modulate the RF signal applied to the piezoelectric disk (blue line). As it can be observed, the time that the signal takes to change from zero to a maximum of transmittance is about 111.6 μs. This time corresponds to the time that the acoustic wave takes to travel along the section of fiber L_2. Furthermore, when the signal is switched off, the transmittance decays from the highest transmittance to zero in a time of 81.7 μs. This decay time corresponds to the time that the acoustic wave takes to travel along section L_1, and therefore the time taken for the coupling between the fundamental core mode and the cladding mode to be eliminated. The red box in the figure indicates a section where steady modulation of

light transmission is observed, after formation of the standing flexural wave. A few periods of modulation extracted from this section are shown in the inset. This amplitude modulation is observed after ~112 μs from the maximum peak transmittance, and is related to the time that takes the acoustic wave to return back along the section of fiber L_2.

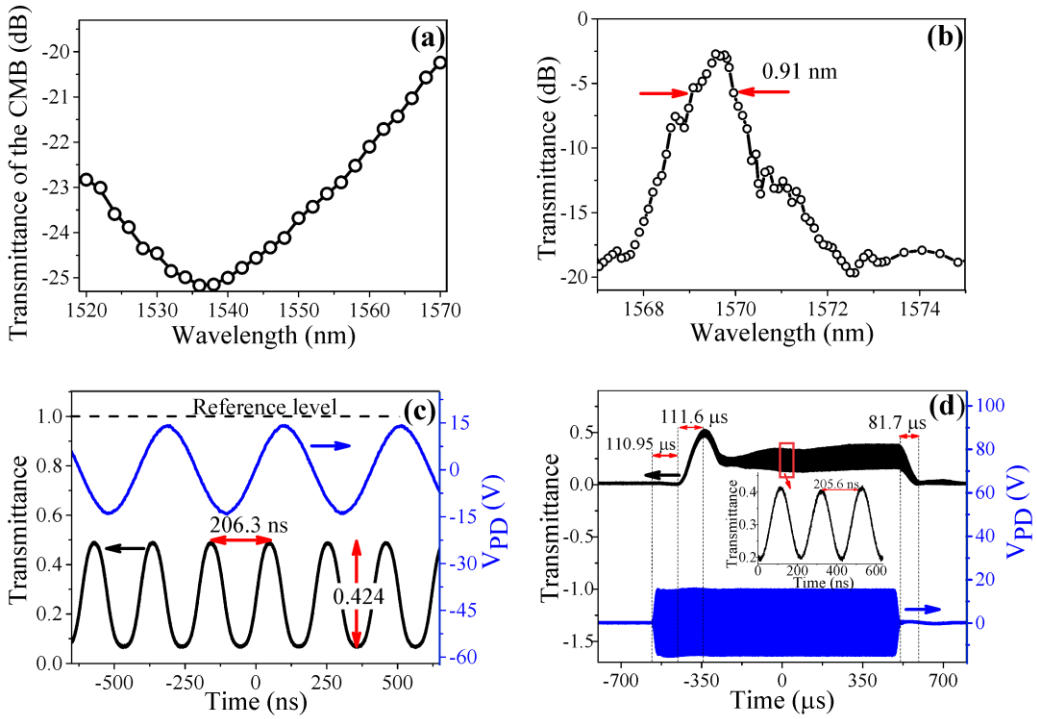

Figure 2. (a) Transmittance of the CMB in the absence of acoustic wave. (b) Maximum transfer of energy at the acoustic frequency of 2.427 MHz. (c) Oscilloscope trace of the AO amplitude modulation recorded at the resonant wavelength of 1569.6 nm. (d) Time response of the AOM, rise and decay times of the optical signal compared with the RF signal. The blue lines in figures (c) and (d) show the RF signal of 28.6 V applied to the piezoelectric disk.

3. The ML and QS pulse regimes

Laser operation in a mode-locked (ML) regime is obtained when the AO modulator is driven to achieve the maximal modulation depth. The acoustic frequency and V_{PZT} were set at 2.427 MHz and 28.6 V, respectively, producing an amplitude modulation at 4.854 MHz. Hence, taking into account an effective index (n_{eff}) of 1.446, the cavity length required to match the laser fundamental frequency with that value is calculated as 42.74 m. However, small errors in the cavity length are expected and these are compensated with a fine adjustment of the acoustic frequency. Stable mode locking operation was obtained at the pump power of 580.3 mW, at the fundamental repetition rate of 4.850836 MHz. The train of mode-locked pulses along with the RF signal applied to the piezoelectric disk are shown in figure 3(a). From this result, one can observe that a pulse train with twice the frequency of the RF signal (2.431614 MHz) is produced. Figure 3(b) shows the corresponding autocorrelation function. The full width at half maximum pulse duration (T_{FWHM}) is measured as 16.73 ps from the full width at half maximum (FWHM) autocorrelation width (T_{ac}) of 25.82 ps (T_{FWHM} = 0.648 T_{ac}), and a maximum peak power of 2.0 W is estimated from the average output power of 186 μW. The measured optical spectrum of the output pulses is shown in figure 3(c). The FWHM of the spectrum (Δλ) is 0.15 nm, centered at 1568.15 nm. The time-bandwidth product is 0.306, close to the ideal transform-limit value of 0.315 for a $Sech^2$ pulse profile.

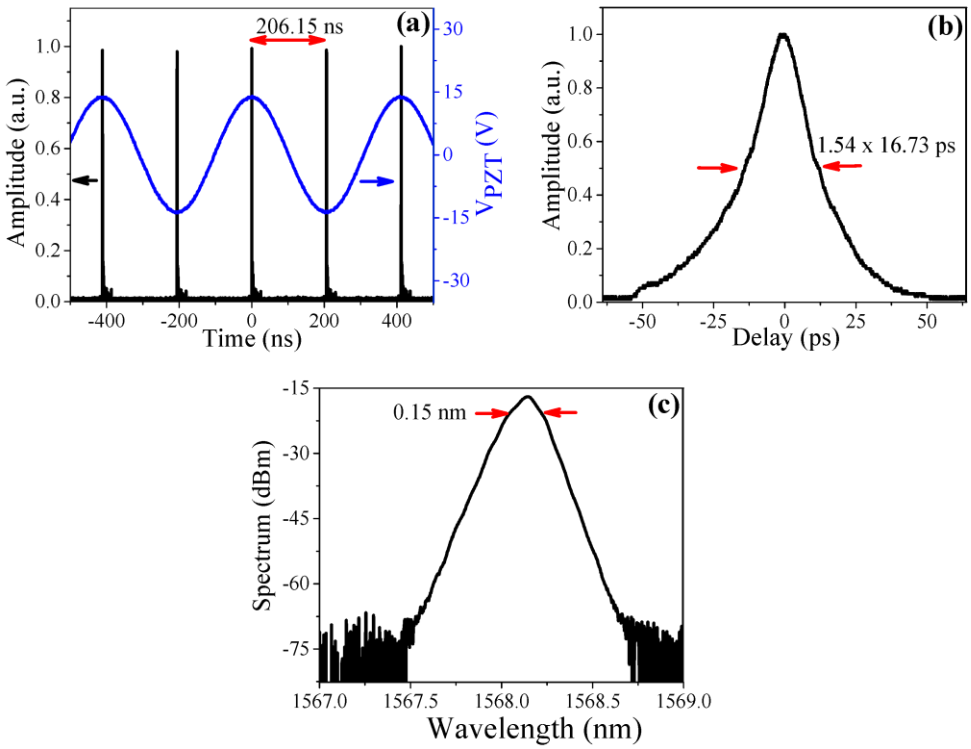

Figure 3. (a) Mode-locked train of pulses generated at 4.850836 MHz with 580.3 mW of pump power. (b) Autocorrelation trace corresponding to output pulses. (c) Measured optical spectrum of the laser.

A change from mode locking operation to a Q-Switching pulsed regime (QS) is realized by superimposing a modulation on the RF signal with a rectangular wave. This modulation produces on-off periods of the acoustic wave that result in a transmittance modulation, see figure 2(d). For this particular case, to obtain a pure Q-switching operation, the RF signal frequency (2.392744 MHz) is slightly detuned to avoid matching between the modulation period and the fundamental cavity round-trip time. For a frequency detuning of 38.87 kHz, a purely Q-switching pulsed operation is obtained when applying a rectangular modulating signal of 1 kHz with a duty cycle of 57% (570 μs "on" periods) at a pump power of 507.3 mW. Figure 4(a) shows the pulse train emitted along with the rectangular modulating signal. The duty cycle of the rectangular signal was adjusted to optimize the amplitude and stability of the Q-switched pulses. Figure 4(b) shows a close-up view of one Q-switched pulse, it exhibits a width of 2.91 μs and a peak power of 852.8 mW. The measured optical spectrum is shown in figure 4(c). The FWHM of the spectrum is 0.095 nm, centered at 1525.86 nm.

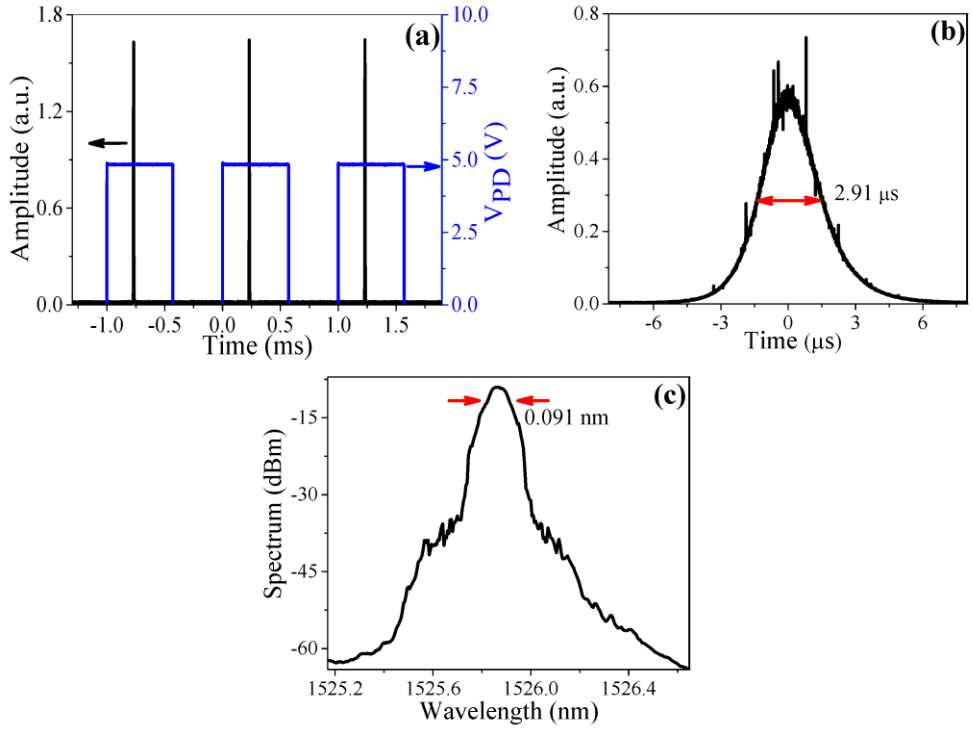

Figure 4. (a) Train of Q-switched pulses generated at 1 kHz of repetition rate with a pump power of 507.3 mW. The blue line corresponds to the rectangular modulation signal. (b) Optical pulse shape showing a pulse width of 2.91 µs and a peak power of 852.8 mW. (c) Measured optical spectrum of the laser.

4. The QML pulse regime

With the objective of producing a simultaneous QML pulse operation, the RF signal frequency was reestablished at 2.431614 MHz, allowing to match the fundamental cavity frequency and to fulfill the mode-locking condition. At the same time, to guarantee an optimum Q-switching behavior, the rectangular modulating signal was fixed at 0.5 kHz, as at this repetition rate best QML performance was obtained. Thus, QML pulsing operation is controlled by variations of the duty cycle. Figure 5(a) shows a close-up view of the highest-intensity Q-switched mode-locked pulse obtained when applying a duty cycle of 52.5% (1.05 ms "on" periods). From this result, it is clearly seen that a Q-switching pulse envelops a train of equally spaced mode-locked sub-pulses. The width (FWHM) of the QML pulse is estimated as 3.5 µs, with a pulse energy of 2.14 µJ and 1.07 mW of average power. Stable QML operation is supported in our setup at duty cycles in a range between 15 and 97.5 %. Figure 5(b) depicts the temporal characteristics of the central ML sub-pulse, measured with a 12.5-GHz detector (Newport 818-BB-51F) and a 20-GHz real-time oscilloscope (Tektronix DPO72004C), see the inset in the figure. Detector measurements reveals a pulse width (FWHM) of 100 ps riding on a broad pedestal of 38.2 ns. Using the relative integral of the oscilloscope trace, the overall energy of the central ML sub-pulse is estimated as 66.4 nJ, from which a pulse energy of 1.48 nJ is approximated for the 100-ps pulse. Therefore, a peak power of 13.90 W is estimated for the central ML sub-pulse. The time interval between ML pulses is measured as 205.95 ns, corresponding with the fundamental cavity round-trip time. The laser linewidth is shown in figure 5(c). The 3-dB optical bandwidth is measured as 0.23 nm, which corresponds to a minimal achievable pulse duration of around 15.68 ps. This discrepancy between experimental and theoretical results might be caused by several factors, one of them could be associated with the relatively short time span over which mode locking develops, reducing significantly the number of cavity round trips required to form a short optical pulse. In addition to this, the time that the acoustic wave takes to travel along the modulator, around 222.6 µs, can be regarded as a long period of time, having a direct impact on the Q switching and mode locking processes. In this respect, it is worth noting that some characteristics of the present device could be further improved by the inclusion of tapered optical fibers, resulting in a more efficient intermodal coupling [26] that leads to improved response times.

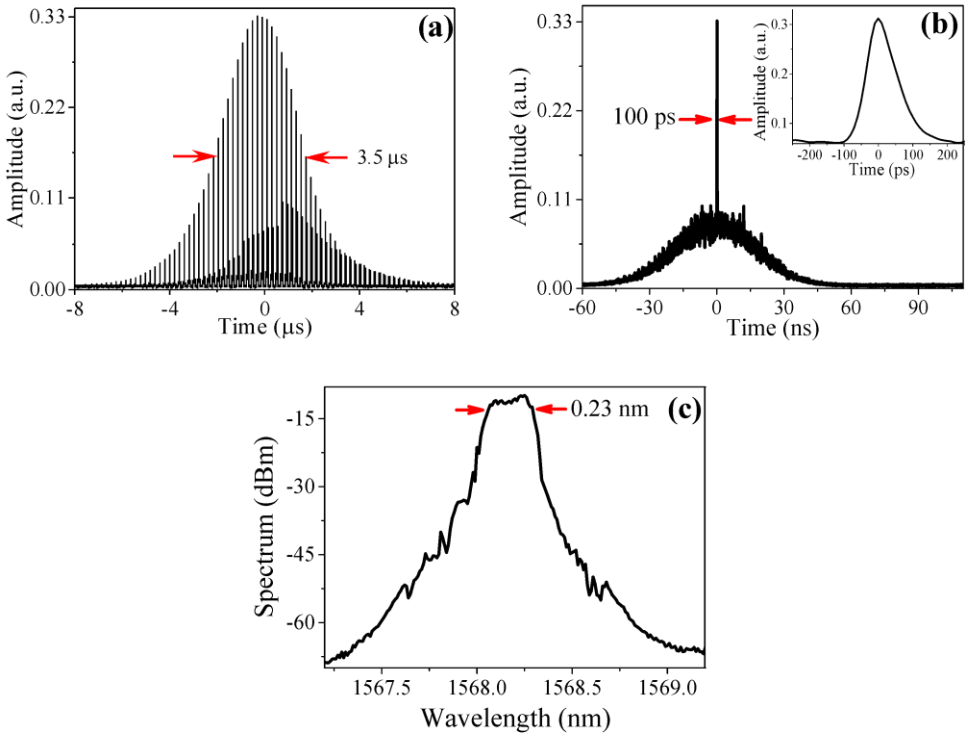

Figure 5. (a) Close-up view of the QML pulse. (b) Measurement of the central ML sub-pulses. (c) Measured optical spectrum in QML operation.

Temporal characteristics of QML pulses as a function of the duty cycle are shown in figure 6(a). For this measurement, both the rectangular modulating signal and the pump power were maintained fixed at 0.5 kHz and 549.2 mW, respectively. This result shows a narrowing of the QML pulse envelope from 4.11 to 3.5 µs as the duty cycle is incremented from 15 to 52.5%, however, further increments in the duty cycle does not induce a further narrowing, but leads to slightly broader light pulses. In contrast, the average power exhibits an opposite behavior, reaching a maximum value of 1.07 mW at 52.5 % of duty cycle. Figure 6(b) shows the performance of the QML pulses as a function of the pump power, by maintaining fixed the repetition rate (0.5 kHz) and duty cycle (52.5%). The QML pulse energy increases with pump power, and there is a corresponding reduction of pulse width, decreasing from 13.58 µs at the lowest pump power, down to 3.5 µs at the maximum pump power available. A maximum overall energy of 2.14 µJ was obtained for the strongest QML pulse, from which a maximum energy of 66.4 nJ is estimated for the central mode-locked sub-pulse.

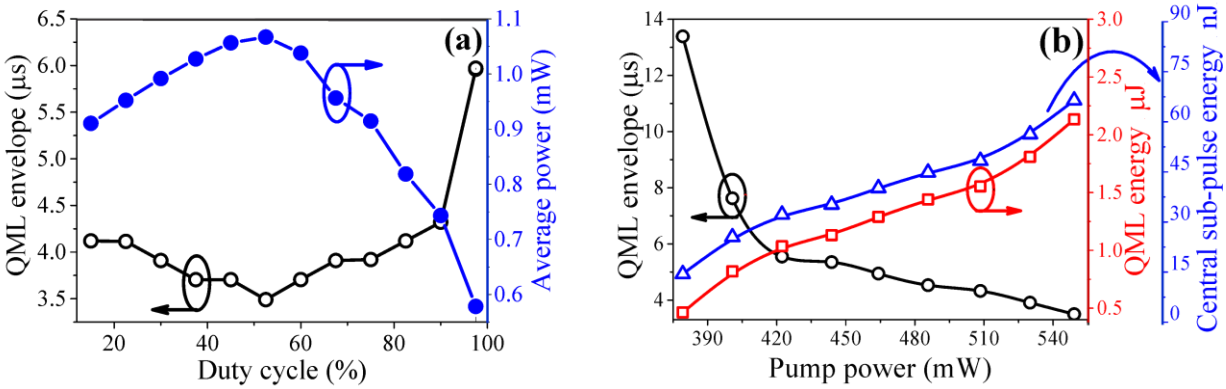

Figure 6. Temporal characteristics of QML pulses. (a) QML envelope and average power as a function of duty cycle at a fixed pump power of 549.2 mW and frequency repetition rate of 0.5 kHz. (b) QML envelope and pulse energy as a function of pump power at the optimum duty cycle of 52.5 % and 0.5 kHz repetition rate.

Compared with similar all-fiber approaches, our scheme possesses the advantages of being a simple structure with an easy fabrication. In addition, the bandpass characteristics of the AO modulator enables laser operation over a wide range of optical wavelengths in conjunction with a short pulse generation, which provides an extra degree of freedom in the laser performance. Improvements on the output pulse characteristics could be feasible by the inclusion of tapered optical fibers in the modulator, leading to a shorter interaction length, faster response times and more stable operation

5. Conclusions

We have reported an experimental investigation regarding a dual actively Q-switched mode-locked all-fiber ring laser by implementing an in-fiber acousto-optic bandpass modulator (AOBM). When the acoustical signal is switched on, a standing flexural acoustic wave is formed on the modulator, and the transmission is amplitude modulated at two times the frequency of the acoustic wave. Therefore, by precisely matching the modulation period and the cavity round-trip time, mode locking condition is satisfied. Simultaneously, by superimposing a rectangular wave modulation on the acoustic signal, intermittent periods of light are generated, allowing control of the Q factor of the cavity. In this manner, the AO modulator performs the double function of active mode locker and Q-switching device. Experimental results demonstrate the potential of the proposed scheme, and provide useful information for future optimization of the AOBM. Best QML pulses were obtained at 0.5 kHz repetition rate, with a pump power of 549.2 mW, at the optical wavelength of 1568.2 nm. A maximum overall energy of 2.14 μJ at an average output power of 1.07 mW was achieved, corresponding to a burst of mode-locked sub-pulses of 100 ps pulse width within a 3.5 μs QML envelope.

Acknowledgments

The authors would like to thanks the funding support by CONACyT “Fronteras de la Ciencia” project 2438 and FAI-UASLP project C18-FAI-05-35.35.

References

[1] Lee H D, Lee J H, Jeong M Y and Kim C S 2011 Characterization of wavelength-swept active mode locking fiber laser based on reflective semiconductor optical amplifier *Opt. Express* **19** 14586–93.

[2] Chen W, Lin W, Qiao T and Yang Z 2015 Additive mode-locked resembling pulses in a Tm-doped fiber laser with a hybrid cavity configuration *Opt. Express* **23** 28012–21.

[3] Minaev V P 2005 Laser apparatus for surgery and force therapy based on high-power semiconductor and fibre lasers Quantum Electron. **35** 976–83.

[4] D. J. Richardson, J. Nilsson, and W. A. Clarkson 2010 High power fiber lasers: current status and future perspectives *J. Opt. Soc. Am. B* **27** B63–92.

[5] Demir A G and Previtali B 2016 Dross-free submerged laser cutting of AZ31 Mg alloy for biodegradable stents *J. Laser Appl*. **28**, 032001
[6] Chang Y M, Lee J, Jhon Y M and Lee J H 2012 Q-switched mode-locking of an erbium-doped fiber laser using cavity modulation frequency detuning *Appl. optics* **51** 5295-301.
[7] Chang Y M, Lee J and Lee J H 2011 A Q-switched, mode-locked fiber laser employing subharmonic cavity modulation *Opt. Express* **19** 26627-33.
[8] Jung M, Lee J, Melkumov M, Khopin V F, Dianov E M and Lee J H 2014 Burst-mode pulse generation from a bismuth-doped germanosilicate fiber laser through self Q-switched mode-locking *Laser Physs Letts.* **11** 125102.
[9] Qiao T, Chen W, Lin W and Yang Z 2016 Generation of Q-switched mode locking controlled rectangular noise-like soliton bunching in a Tm-doped fiber laser *Opt. Express* **24** 18755-63.
[10] Chang W C, Lin Y S, Lee Y W, Chen C H, Lin J H, Reddy P H, Das S, Dhar A and Paul M C 2017 Investigation of Q-switched and mode-locked pulses from a Yb^{3+}-doped germano-zirconia silica glass based fiber laser *IEEE Photonics Journal* **9** 1-8
[11] Yang X and Yang C X 2009 Q-switched mode-locking in an erbium-doped femtosecond fiber laser based on nonlinear polarization rotation *Laser Phys.* **19** 2106–9.
[12] Lin K H, Kang J J, Wu H H, Lee C K and Lin G R 2009 Manipulation of operation states by polarization control in an erbium-doped fiber laser with a hybrid saturable absorber *Opt. Express* **17** 4806–14
[13] Jun C S and Kim B Y2011 Mode-locking and Q-switching in multi-wavelength fiber ring laser using low frequency phase modulation *Opt. Express* **19** 6290–5.
[14] Wang S, Rhee H, Wang X, Eichler H J, Meister S, Riesbeck T and Chen J 2010 LD end pumped, actively mode locked and passively Q-switched Nd: YAP laser at 1341 nm *Opt. Commun.* **283** 570-3.
[15] Lee J, Koo J, Chang Y M, Debnath P, Song Y W and Lee J H 2012 Experimental investigation on a Q-switched, mode-locked fiber laser based on the combination of active mode locking and passive Q switching *JOSA* B **29** 1479-85.
[16] Kong L C, Xie G Q, Yuan P, Qian L J, Wang S X, Yu H H and Zhang H J 2015 Passive Q-switching and Q-switched mode-locking operations of 2 mm Tm:CLNGG laser with MoS_2 saturable absorber mirror *Photon. Res.* **3** A47-50.
[17] Chen Y F and Tsai S W 2011 Simultaneous Q-switching and mode-locking in a diode-pumped Nd:YVO_4-Cr^{4+}:YAG laser *IEEE J. Quantum Electron.* **37** 580–6.
[18] Theobald C, Weitz M, Knappe R, Wallenstein R and L'Huillier J A 2008 Stable Q-switch mode-locking of Nd:YVO4 lasers with a semiconductor saturable absorber *Appl. Phys.* B **92** 1–3.
[19] Cuadrado Laborde C, Díez A, Cruz J L and Andrés M V 2009 Doubly active Q-switching and mode locking of an all-fiber laser *Opt. Lett.* **34** 2709–11 2009.
[20] Chang Y M, Lee J and Lee J H 2011 A Q-switched, mode-locked fiber laser employing subharmonic cavity modulation *Opt. Express* **19** 26627–63.
[21] Datta P K, Mukhopadhyay S, Das S K, Tartara L, Agnesi A and Degiorgio V 2004 Enhancement of stability and efficiency of a nonlinear mirror mode-locked Nd: YVO_4 oscillator by an active Q-switch *Opt. Express* **12** 4041-6.
[22] Li M, Zhao S, Yang K, Li G, Li D, Wang J, Jing A and Qiao W 2008 Actively Q-switched and Mode-Locked Diode-Pumped Nd:$GdVO_4$-Laser *IEEE Journal of Quantum Electronics* **44** 288-93.
[23] Zhao S, Li G, Li D, Yang K, Li Y, Li M, Li T, Zhang G and Cheng K 2010 Numerical simulation of dual-loss-modulated Q-switched and mode-locked laser with an acousto-optic and Cr^{4+}:YAG saturable absorber *Appl. Opt.* **49** 1802–8.
[24] Cuadrado Laborde C, Diez A, Delgado Pinar M, Cruz J L and Andrés M V 2009 Mode locking of an all-fiber laser by acousto-optic superlattice modulation *Opt. Lett.* **34** 1111-3.
[25] Ramírez Meléndez G, Bello Jiménez M, Pottiez O and Andrés M V 2017 Improved All-Fiber Acousto-Optic Tunable Bandpass Filter *IEEE Photon. Technol. Lett.* **29** 1015-8.
[26] Bello Jiménez M, Cuadrado Laborde C, Diez A, Cruz J L, Andrés M V and Rodríguez Cobos A 2013 Mode-locked all-fiber ring laser based on broad bandwidth in-fiber acousto-optic modulator *Appl. Phys.* B **110** 73-80.
[27] Delgado Pinar M, Zalvidea D, Diez A, Pérez Millán P and Andrés M V 2006 Q-switching of an all-fiber laser by acousto-optic modulation of a fiber Bragg grating *Opt. Express* **14**, 1106-12.
[28] Bello Jiménez M, Cuadrado Laborde C, Sáez Rodríguez D, Díez A, Cruz J L and Andrés M V 2010 Actively mode-locked fiber ring laser by intermodal acousto-optic modulation *Opt. Lett.* **35** 3781–3.
[29] Cuadrado Laborde C, Díez A, Cruz J L and Andrés M V 2010 Experimental study of an all-fiber laser actively mode locked by standing-wave acousto-optic modulation *Appl. Phys.* B **99** 95–9.

[30] Kim J, Koo J and Lee J H 2017 All-fiber acousto-optic modulator based on a cladding-etched optical fiber for active mode-locking *Photon. Res* **5** 391-5.

[31] Ramirez Meléndez G, Bello Jiménez M, Pottiez O, Escalante Zarate L, López Estopier R, Ibarra Escamilla B, Durán Sánchez M, Kuzin E A and Andrés M V 2017 Q-switching of an all-fiber ring laser based on in-fiber acousto-optic bandpass modulator *Appl. Phys.* B **123**, 249.

[32] Bello Jiménez M, Hernández Escobar E, Camarillo Avilés A, Pottiez O, Díez A and Andrés M V 2018 Actively mode-locked all-fiber laser by 5 MHz transmittance modulation of an acousto-optic tunable bandpass filter *Laser Phys. Letts*. **15** 085113.